

Insertion of CO and Alkenes into the (methyl)Pd Complexes of the Bidentate Porphyrin Ligand

Jun-ichiro Setsune,* Takashi Yamauchi, Sachiko Tanikawa, Yuka Hirose, and Jun-ya Watanabe

Department of Chemistry, Faculty of Science, and Graduate School of Science and Technology, Kobe University, Nada-ku, Kobe 657-8501, Japan

Received March 27, 2004

The (methyl)Pd complex of a bidentate N^{21},N^{22} -1,2-diphenyletheno-bridged porphyrin ligand, $\text{Pd}^{\text{II}}(\text{Me})(\text{Cl})(N^{21},N^{22}\text{-(PhC=CPh)}(\text{TPP}))$, gave the (acetyl)Pd complex $\text{Pd}^{\text{II}}(\text{C(O)Me})(\text{Cl})(N^{21},N^{22}\text{-(PhC=CPh)}(\text{TPP}))$ in 85% yield under atmospheric CO pressure. The acetyl–chloro site exchange in the (acetyl)Pd complex was monitored by variable-temperature NMR, and the ΔG^\ddagger_{323} value was estimated as 68 kJ mol⁻¹. The reaction of the cationic (methyl)Pd complex $[\text{Pd}^{\text{II}}(\text{Me})(N^{21},N^{22}\text{-(PhC=CPh)}(\text{TPP}))(\text{MeCN})]\text{ClO}_4$ with CO gave a cationic (acetyl)-(carbonyl)Pd complex which readily lost CO to give the (carbonyl)(methyl)Pd complex $[\text{Pd}^{\text{II}}(\text{Me})(N^{21},N^{22}\text{-(PhC=CPh)}(\text{TPP}))(\text{CO})]\text{ClO}_4$. These Pd complexes were easily characterized by the ¹H NMR spectra. The X-ray crystal structures of the (acetyl)Pd complex and the (carbonyl)(methyl)Pd complexes were determined. Insertion of norbornadiene and norbornene into the cationic (carbonyl)(methyl)Pd complex occurred on the exo side. Two isomers with different orientations of the norbornenyl moiety relative to the bidentate porphyrin ligand were observed at low temperature, and isomerization by a ligand rotation mechanism occurred at room temperature to give a single isomer.

Introduction

The insertion of unsaturated compounds to the (methyl)Pd complexes is regarded as one of the most fundamental organometallic reactions and attracting great interest as a basis for the Pd-catalyzed polymerizations of alkenes with a functional substituent and for the Pd-catalyzed copolymerizations between CO and alkenes, which leads to high-performance polymer materials.¹ Since the reactivity and stability of the (alkyl)Pd and (acyl)Pd complexes are governed by the auxiliary bidentate ligands, the insertion reactions of CO and alkene into the Pd–C bond have been investigated by using various bidentate ligands such as those having P–P, N–P, and N–N coordinating atoms.^{2–4} The molecular architecture of the bidentate ligands is also

very important, as it has been shown that the steric bulkiness above and below the square plane of Pd retards the associative ligand exchange process to lead to the formation of high-molecular-weight polymers.^{4b}

It is well-known that the electronic and steric properties of the porphyrin ligand govern the structures and reactions of metallocporphyrins,⁵ and we have recently developed novel bidentate porphyrins that can be used for the square-planar Pd(II) complexes.⁶ One of the two faces of the square plane of the Pd coordination is completely covered by this bidentate porphyrin. Since the other two ligands on Pd are very close to the porphyrin ring, their reactions are affected by the bidentate porphyrin ligand. Therefore, it is of interest to investigate the insertion reactions of CO and alkenes into the (methyl)Pd complexes of the bidentate porphyrin ligand. We describe here the structure and reaction of the (methyl)Pd and (acetyl)Pd complexes of porphyrin with a N^{21},N^{22} bridging group. The influence of this bidentate porphyrin ligand on the Pd chemistry is

* To whom correspondence should be addressed. Phone: +81-78-803-5683. Fax: +81-78-803-5770. E-mail: setsunej@kobe-u.ac.jp.

(1) (a) Ittel, S. D.; Johnson, L. K.; Brookhart, M. *Chem. Rev.* **2000**, *100*, 1169. (b) Mecking, S. *Coord. Chem. Rev.* **2000**, *203*, 325. (c) Gibson, V. C.; Spitzmesser, S. K. *Chem. Rev.* **2003**, *103*, 283. (d) Schmid, M.; Eberhardt, R.; Klinga, M.; Leskelä, M.; Rieger, B. *Organometallics* **2001**, *20*, 2321.

(2) (a) Dekker, G. P. C. M.; Elsevier, C. J.; Vrieze, K.; van Leeuwen, P. W. N. M. *Organometallics* **1992**, *11*, 1598. (b) Tóth, I.; Elsevier, C. J. *J. Am. Chem. Soc.* **1993**, *115*, 10388. (c) Nozaki, K.; Sato, N.; Takaya, H. *J. Am. Chem. Soc.* **1995**, *117*, 9911. (d) Koide, Y.; Bott, S. G.; Barron, A. R. *Organometallics* **1996**, *15*, 2213.

(3) (a) Dekker, G. P. C. M.; Buijs, A.; Elsevier, C. J.; Vrieze, K.; Van Leeuwen, P. W. N. M.; Smeets, W. J. J.; Spek, A. L.; Wang, Y. F.; Stam, C. H. *Organometallics* **1992**, *11*, 1937. (b) Rülke, R. E.; Kaasjager, V. E.; Wehman, P.; Elsevier, C. J.; van Leeuwen, P. W. N. M.; Vrieze, K.; Fraanje, J.; Goubitz, K.; Spek, A. L. *Organometallics* **1996**, *15*, 3022. (c) Ankersmit, H. A.; Veldman, N.; Spek, A. L.; Eriksen, K.; Goubitz, K.; Vrieze, K.; van Koten, G. *Inorg. Chim. Acta* **1996**, *252*, 203. (d) Luinstra, G. A.; Brinkmann, P. H. P. *Organometallics* **1998**, *17*, 5160. (e) Reddy, K. R.; Surekha, K.; Lee, G.-H.; Peng, S.-M.; Chen, J.-T.; Liu, S.-T. *Organometallics* **2000**, *20*, 1292. (f) Daugulis, O.; Brookhart, M. *Organometallics* **2002**, *21*, 5926.

(4) (a) Byers, P. K.; Canty, A. J. *Organometallics* **1990**, *9*, 210. (b) de Graaf, W.; Boersma, J.; van Koten, G. *Organometallics* **1990**, *9*, 1479. (c) Johnson, L. K.; Killiam, C. M.; Brookhart, M. *J. Am. Chem. Soc.* **1995**, *117*, 6414. (d) Markies, B. A.; Wijkens, P.; Dedieu, A.; Boersma, J.; Spek, A. L.; van Koten, G. *Organometallics* **1995**, *14*, 5628. (e) Salo, E. V.; Guan, Z. *Organometallics* **2003**, *22*, 5033.

(5) (a) Sanders, J. K. M.; Bampos, N.; Clyde-Watson, Z.; Darling, S. L.; Hawley, J. C.; Kim, H.-J.; Mak, C. C.; Webb, S. J. In *The Porphyrin Handbook*; Kadish, K. M., Smith, K. M., Guillard, R., Eds.; Academic Press: San Diego, CA, 1999; Vol. 3, pp 1–48. (b) Scheidt, W. R. In *The Porphyrin Handbook*; Kadish, K. M., Smith, K. M., Guillard, R., Eds.; Academic Press: San Diego, CA, 1999; Vol. 3, pp 49–112.

(6) (a) Takao, Y.; Takeda, T.; Miyashita, K.; Setsune, J. *Chem. Lett.* **1996**, 761. (b) Takao, Y.; Takeda, T.; Setsune, J. *Bull. Chem. Soc. Jpn.* **1998**, *71*, 1327. (c) Takao, Y.; Takeda, T.; Watanabe, J.; Setsune, J. *Organometallics* **1999**, *18*, 2936. (d) Takao, Y.; Takeda, T.; Watanabe, J.; Setsune, J. *Organometallics* **2003**, *22*, 233. (e) Takao, Y.; Takeda, T.; Setsune, J. *Bull. Chem. Soc. Jpn.* **2003**, *76*, 1549.

illustrated by the remarkable thermodynamic stability of the cationic (carbonyl)(methyl)Pd complex over the (acetyl)(carbonyl)Pd complex.

Experimental Section

General Considerations. The bridged porphyrin free base $N^{21}N^{22}$ -(PhC=CPh)(TPP) (**1**)^{6b} and Pd(Me)(Cl)(cyclooctadiene) were synthesized according to the literature methods.⁷ Solvents were purified prior to use by conventional methods. CDCl₃ was passed through basic Al₂O₃ before use. Other chemicals were of reagent grade and used as received. Wakogel C-300 silica gel (Wako Junyaku) was used for column chromatography. ¹H NMR was recorded on a Varian Inova 400 spectrometer. Chemical shifts were referenced with respect to (CH₃)₄Si (0 ppm) as an internal standard. The UV–visible spectra were measured on a Jasco V-570 spectrometer. Elemental analyses of C, H, and N were made with a Yanaco MT-5 CHN recorder. ESI-MS spectra were measured with a Mariner PE Biosystems instrument. The compounds prepared here are perchlorates that could involve risk of an explosion and must be handled with extreme caution.

Pd^{II}(Me)(Cl)(N²¹,N²²-(PhC=CPh)(TPP)) (2). A mixture of the bridged porphyrin free base $N^{21}N^{22}$ -(PhC=CPh)(TPP) (**1**; 552 mg, 6.98 × 10⁻⁴ mol) and Pd(Me)(Cl)(cyclooctadiene) (185 mg, 6.98 × 10⁻⁴ mol) in 50 mL of benzene was stirred at room temperature for 1 h. The solvent was removed under reduced pressure, and the residue was chromatographed on silica gel. The fraction that eluted with dichloromethane/acetone (20/1 to 10/1) was collected to give a brown powder (617 mg, 6.51 × 10⁻⁴ mol) of the product after precipitation from dichloromethane/hexane. **2**: yield 93%. ¹H NMR (δ, CDCl₃): 8.93, 8.87, 8.67, 8.53, 8.47, 8.07 (d × 6, 1H × 6, pyrrole β-H, J_{vic} = 4.8 Hz); 8.47 (m, 2H, pyrrole β-H); 8.5–7.2 (m, 20H, *meso* Ph H); 6.15, 6.13 (t × 2, 1H × 2, bridge Ph *p*-H); 5.76 (br, 4H, bridge Ph *m*-H); -4.13 (s, 3H, Pd-Me). UV/vis (CH₂Cl₂; λ_{max}, nm (log ε)): 414 (4.77), 458 (sh) (4.65), 562 (3.79), 652 (3.75), 692 (3.78). Anal. Calcd for C₅₉H₄₁ClN₄Pd·½C₆H₁₀O·2H₂O: C, 71.76; H, 4.94; N, 5.49. Found: C, 71.45; H, 5.10; N, 5.36. MS (ESI-TOF in MeOH; *m/z*): 911.18 (calcd for C₅₉H₄₁N₄-Pd (M - Cl)⁺ 911.24).

[Pd^{II}(Me)(Cl)(N²¹,N²²-(PhC=CPh)(TPP))(MeCN)]ClO₄ (3). A mixture of Pd^{II}(Me)(Cl)(N²¹,N²²-(PhC=CPh)(TPP)) (**2**; 101 mg, 1.07 × 10⁻⁴ mol), AgClO₄ (22.2 mg, 1.07 × 10⁻⁴ mol), dichloromethane (15 mL), and acetonitrile (15 mL) was stirred at room temperature for 1 h. After AgCl was filtered off, the solvents were removed under reduced pressure. The residue was purified by precipitation from dichloromethane/hexane to give a green powder (108.6 mg, 1.03 × 10⁻⁴ mol) of the product. **3**: yield 97%. ¹H NMR (δ, CDCl₃): 9.45, 9.00, 8.85, 8.80, 8.61, 8.60, 8.19, 8.05 (d × 8, 1H × 8, pyrrole β-H, J_{vic} = 4.4–5.2 Hz); 8.4–7.2 (m, 20H, *meso* Ph H); 6.19, 6.17 (t × 2, 1H × 2, bridge Ph *p*-H); 5.79 (br, 4H, bridge Ph *m*-H); 0.96 (s, 3H, Pd-NCMe); -4.35 (s, 3H, Pd-Me). UV/vis (CH₂Cl₂; λ_{max}, nm (log ε)): 416 (sh) (4.67), 468 (4.87), 580 (3.81), 636 (3.96), 676 (3.90) nm. Anal. Calcd for C₆₁H₄₄ClN₅O₄Pd·½H₂O: C, 66.73; H, 4.50; N, 6.38. Found: C, 66.63; H, 4.58; N, 6.23. MS (ESI-TOF in MeOH; *m/z*): 911.17 (calcd for C₆₁H₄₄N₅Pd (M - ClO₄ - CH₃CN)⁺ 911.24).

Pd^{II}(C(O)Me)(Cl)(N²¹,N²²-(PhC=CPh)(TPP)) (4). A 200 mL balloon filled with CO gas was connected to a flask containing a dichloromethane solution (10 mL) of Pd^{II}(Me)(Cl)(N²¹,N²²-(PhC=CPh)(TPP)) (**2**; 74.2 mg, 7.83 × 10⁻⁵ mol). The flask was immersed in an ice bath, and the solution was vigorously stirred for 1 h. The solvent was removed under reduced pressure, and the residue was purified by precipitation from dichloromethane/hexane to give a brown powder (71.0 mg, 7.28 × 10⁻⁵ mol) of the product. **4**: yield 93%. ¹H NMR

(δ, CDCl₃): 9.07, 8.94, 8.67, 8.64, 8.50, 8.49, 8.07, 8.02 (d × 8, 1H × 8, pyrrole β-H, J = 4.6–5.0 Hz); 8.4–7.0 (m, 20H, *meso* Ph H); 6.15 (br, 2H, bridge Ph *p*-H); 5.75 (br, 4H, bridge Ph *m*-H); -1.27 (s, 3H, Pd-COMe). UV/vis (CH₂Cl₂; λ_{max}, nm (log ε)): 412 (sh) (4.68), 458 (4.87), 560 (3.92), 620 (3.88), 668 (3.75). Anal. Calcd for C₆₀H₄₁ClN₄OPd·C₄H₁₀O·½H₂O: C, 72.59; H, 4.95; N, 5.29. Found: C, 72.42; H, 5.00; N, 5.48. MS (ESI-TOF in MeOH): *m/z* 939.17 (calcd for C₆₀H₄₁N₄OPd (M - Cl)⁺ 939.23).

[Pd^{II}(Me)(N²¹,N²²-(PhC=CPh)(TPP))(CO)]ClO₄ (5). A 200 mL balloon filled with CO gas was connected to a flask containing a dichloromethane solution (5 mL) of [Pd^{II}(Me)(N²¹,N²²-(PhC=CPh)(TPP))(MeCN)]ClO₄ (**3**; 44.5 mg, 4.23 × 10⁻⁵ mol). The flask was immersed in an ice bath, and the solution was vigorously stirred for 1 h. The solvent was removed under reduced pressure, and the residue was purified by precipitation from dichloromethane/hexane to give a green powder (42.0 mg, 4.04 × 10⁻⁵ mol) of the product. **5**: yield 96%. ¹H NMR (δ, CDCl₃): 9.27, 9.22, 8.95, 8.86, 8.82, 8.80, 8.33, 8.26 (d × 8, 1H × 8, pyrrole β-H, J = 4.5–5.1 Hz); 8.4–7.0 (m, 20H, *meso* Ph H); 6.23 (t × 2, 1H × 2, bridge Ph *p*-H); 5.83 (br, 4H, bridge Ph *m*-H); -4.06 (s, 3H, Pd-Me). UV/vis (CH₂Cl₂; λ_{max}, nm (log ε)): 402 (4.46), 462 (5.01), 574 (3.82), 620 (3.96), 658 (3.90) nm. IR (KBr): 2099 cm⁻¹ (CO). Anal. Calcd for C₆₀H₄₁ClN₄O₅Pd·½H₂O: C, 66.43; H, 4.27; N, 5.16. Found: C, 66.44; H, 4.32; N, 5.25. MS (ESI-TOF in MeOH; *m/z*): 939.17 (calcd for C₆₀H₄₁N₄OPd (M - ClO₄)⁺ 939.23).

Pd(C₇H₈C(O)CH₃)(Cl)(N²¹,N²²-(PhC=CPh)(TPP)) (11). A mixture of Pd^{II}(C(O)Me)(Cl)(N²¹,N²²-(PhC=CPh)(TPP)) (**4**; 11.8 mg, 1.21 × 10⁻⁵ mol) and norbornadiene (11.1 mg, 1.28 × 10⁻⁴ mol) dissolved in chloroform (0.5 mL) was stirred for 14 h at room temperature. Repeated precipitation from dichloromethane/hexane afforded a brown powder (11.7 mg, 1.10 × 10⁻⁵ mol) of the product. **11**: yield 96%. ¹H NMR (δ, CDCl₃): 9.08, 8.96, 8.85, 8.77, 8.65, 8.57, 8.22, 8.21 (d × 8, 1H × 8, J = 4.4–5.2 Hz, β py H); 7.15–8.39 (m, 20H, *meso* Ph H); 6.23 (t, 2H, bridge Ph *p*-H); 5.83 (br, 4H, bridge Ph *m*-H); 5.04, 4.97 (dd × 2, 1H × 2, J = 5.6 Hz, J = 2.8 Hz, vinyl); 1.49, -0.29 (s × 2, 1H × 2, bridgehead CH); 0.58 (s, 3H, C(O)CH₃); -0.07 (d, 1H, J = 8.4 Hz, bridge CH₂); -0.69 (d, 1H, J = 6.4 Hz, Pd-CHCHC(O)Me); -0.88 (d, 1H, J = 8.4 Hz, bridge CH₂); -4.48 (dd, 1H, J = 6.4 Hz, J = 2.4 Hz, Pd-CH-). UV/vis (CH₂Cl₂; λ_{max}, nm (log ε)): 414 (sh) (4.69), 460 (4.71), 564 (sh) (3.93), 648 (4.02), 676 (4.05). IR (KBr): 1700, 1624, 1598, 1574 cm⁻¹ (carbonyl). Anal. Calcd for C₆₇H₄₉N₄OCIPd·3H₂O: C, 72.00; H, 4.94; N, 5.04. Found: C, 71.72; H, 4.94; N, 4.99. MS (ESI-TOF in MeOH; *m/z*): 1031.25 (calcd for C₆₇H₄₉N₄OPd (M - Cl)⁺ 1031.30).

Pd(C₇H₁₀C(O)CH₃)(Cl)(N²¹,N²²-(PhC=CPh)(TPP)) (12). A mixture of Pd^{II}(C(O)Me)(Cl)(N²¹,N²²-(PhC=CPh)(TPP)) (**4**; 13.8 mg, 1.41 × 10⁻⁵ mol) and norbornene (4 mg, 4.2 × 10⁻⁵ mol) dissolved in chloroform (0.5 mL) was stirred for 36 h at room temperature. Repeated precipitation from dichloromethane/hexane afforded a brown powder (12.2 mg, 1.10 × 10⁻⁵ mol) of the product. **12**: yield 81%. ¹H NMR (δ, CDCl₃): 9.14, 8.96, 8.85, 8.74, 8.72, 8.55, 8.20, 8.18 (d × 8, 1H × 8, J = 4.4–5.2 Hz, β py H); 7.15–8.42 (m, 20H, *meso* Ph H); 6.22 (m, 2H, bridge Ph *p*-H); 5.83 (br, 4H, bridge Ph *m*-H); 0.60, 0.42 (m × 2, 1H × 2, *exo*-CH₂-); 0.02, -0.35 (m × 2, 1H × 2, *endo*-CH₂-); 0.84, -1.07 (s × 2, 1H × 2, bridge CH); 0.58 (s, 3H, C(O)Me); -0.19 (d, 1H, J = 8.6 Hz, bridge CH₂); -0.51 (d, 1H, J = 6.4 Hz, Pd-CHCHCOME); -0.69 (d, 1H, J = 8.6 Hz, bridge CH₂); -4.05 (dd, 1H, J = 6.4 Hz, J = 2.4 Hz, Pd-CH-). UV/vis (CH₂Cl₂; λ_{max}, nm (log ε)): 410 (sh) (4.71), 454 (4.78), 562 (3.90), 646 (3.96), 678 (3.98). IR (KBr; cm⁻¹): 1704, 1612, 1598, 1576 (carbonyl). Anal. Calcd for C₆₇H₅₁N₄OCIPd·½H₂O·2CH₂Cl₂: C, 66.35; H, 4.52; N, 4.49. Found: C, 66.45; H, 4.55; N, 4.81. MS (ESI-TOF in MeOH; *m/z*): 1033.26 (calcd for C₆₇H₅₁N₄OPd (M - Cl) 1033.31).

[Pd(C₇H₈C(O)CH₃)(N²¹,N²²-(PhC=CPh)(TPP))]ClO₄ (13a). A chloroform solution of norbornadiene (8.8 μL of a 6.0 M

(7) Rülke, R. E.; Ernsting, J. M.; Spek, A. L.; Elsevier, C. J.; van Leeuwen, P. W. N. M.; Vrieze, K. *Inorg. Chem.* **1993**, *32*, 5769.

solution) was added to a chloroform solution (0.5 mL) of $[\text{Pd}^{\text{II}}(\text{Me})(N^{21},N^{22}-(\text{PhC}=\text{CPh})(\text{TPP}))(\text{CO})]\text{ClO}_4$ (**5**; 11.1 mg, 1.05×10^{-5} mol) at room temperature. Solvent was removed after 3.5 h, and then repeated precipitation from dichloromethane/hexane afforded a green powder (10.6 mg, 9.50×10^{-6} mol) of the product. **13a**: yield 91%. ^1H NMR (δ , CDCl_3): 9.09, 9.03, 8.84, 8.76, 8.64, 8.57, 8.22, 8.21 (d \times 8, 1H \times 8, $J = 4.9$ – 5.2 Hz, β py H); 7.15–8.48 (m, 20H, *meso* Ph H); 6.22 (m, 2H, bridge Ph *p*-H); 5.83 (br, 4H, bridge Ph *m*-H); 5.06, 4.95 (dd \times 2, 1H \times 2, $J = 5.6$ Hz, $J = 2.8$ Hz); 1.48, -0.31 (s \times 2, 1H \times 2, bridgehead CH); 0.58 (s, 3H, C(O)CH₃); -0.11 (d, 1H, $J = 7.3$ Hz, bridge CH₂); -0.61 (d, 1H, $J = 6.4$ Hz, Pd–CHCH–COMe); -0.91 (d, 1H, $J = 8.5$ Hz, bridge CH₂); -4.51 (dd, 1H, $J = 6.2$ Hz, $J = 2.2$ Hz, Pd–CH–). UV/vis (CH_2Cl_2 ; λ_{max} , nm (log ϵ): 412 (sh) (4.72), 452 (4.81), 564 (3.73), 636 (3.84), 682 (3.88). IR (KBr; cm^{-1}): 1710, 1612, 1576 (carbonyl). Anal. Calcd for $\text{C}_{67}\text{H}_{49}\text{N}_4\text{O}_5\text{ClPd}\cdot 2\text{H}_2\text{O}$: C, 68.90; H, 4.57; N, 4.80. Found: C, 69.12; H, 4.74; N, 4.72. MS (ESI-TOF in MeOH; m/z): 1031.22 (calcd for $\text{C}_{67}\text{H}_{49}\text{N}_4\text{O}_5\text{Pd}(\text{M} - \text{ClO}_4)^+$ 1031.30).

A CDCl_3 solution of norbornadiene (6 μL of a 6.0 M solution) was added to a cooled CDCl_3 solution (0.5 mL) of $[\text{Pd}^{\text{II}}(\text{Me})(N^{21},N^{22}-(\text{PhC}=\text{CPh})(\text{TPP}))(\text{CO})]\text{ClO}_4$ (**5**; 6.8 mg, 6.54×10^{-5} mol), and this sample tube was immediately put into the NMR probe cooled at -50 °C in advance. After 10 min at -50 °C the ^1H NMR showed signals due to **13b** in addition to **13a**. Data for **13b** are as follows. ^1H NMR (δ , CDCl_3 , 0 °C): 9.25, 8.96, 8.86, 8.85, 8.68, 8.50, 8.19, 8.13 (d \times 8, 1H \times 8, $J = 4.8$ – 5.1 Hz, β py H); 7.09–8.48 (m, 20H, *meso* Ph H); 5.04, 4.77 (m, 1H \times 2, vinyl); 1.42, -2.11 (s \times 2, 1H \times 2, bridgehead); 0.82 (s, 3H, C(O)CH₃); 0.15 (d, 1H, $J = 6.4$ Hz, Pd–CHCH–(O)Me); -0.95 (d, 1H, $J = 8.0$ Hz, bridge CH₂); -1.69 (dd, 1H, $J = 6.1$ Hz, $J = 2.1$ Hz, Pd–CH–); -3.82 (d, 1H, $J = 8.1$ Hz, bridge CH₂).

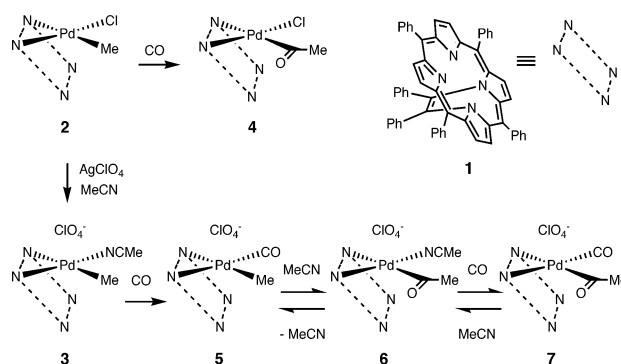
[Pd₂(C₇H₈(C(O)CH₃)₂(N²¹,N²²-(PhC=CPh)(TPP))₂](ClO₄)₂ (14**)**. A chloroform solution of norbornadiene (25 μL of a 0.16 M solution) was added to a chloroform solution (0.5 mL) of $[\text{Pd}^{\text{II}}(\text{Me})(N^{21},N^{22}-(\text{PhC}=\text{CPh})(\text{TPP}))(\text{CO})]\text{ClO}_4$ (**5**; 8.5 mg, 8.17×10^{-6} mol) at room temperature, and the reaction mixture was allowed to stand for 1 h. Repeated precipitation from dichloromethane/hexane afforded a green powder (7.4 mg, 3.75×10^{-6} mol) of the product. **14**: yield 92%. ^1H NMR (δ , CDCl_3): 9.11, 8.91, 8.59, 8.53, 8.44, 8.36, 8.04, 7.77 (d \times 8, 1H \times 8, $J = 4.6$ – 5.6 Hz, β py H); 7.15–8.76 (m, 20H, *meso* Ph H); 6.51 (t, 2H, bridge Ph *p*-H); 5.80 (br, 4H, bridge Ph *m*-H); 0.21 (s, 3H, C(O)CH₃); -1.70 (d, 2H, $J = 6.4$ Hz, Pd–CHCHCOMe); -1.81 (s, 2H, bridgehead); -2.65 (s, 2H, bridge); -4.59 (d, 2H, $J = 6.2$ Hz, Pd–CH–). UV/vis (CH_2Cl_2 ; λ_{max} , nm (log ϵ): 412 (sh) (5.07), 450 (5.14), 572 (4.06), 634 (4.20), 668 (4.23). IR (KBr; cm^{-1}): 1612, 1574 (carbonyl). Anal. Calcd for $\text{C}_{127}\text{H}_{90}\text{N}_8\text{O}_{10}\text{Cl}_2\text{Pd}_2\cdot 2\text{H}_2\text{O}$: C, 69.09; H, 4.29; N, 5.08. Found: C, 68.85; H, 4.50; N, 4.91. MS (ESI-TOF in MeOH; m/z): 986.17 (calcd for $\text{C}_{127}\text{H}_{90}\text{N}_8\text{O}_{10}\text{Pd}_2(\text{M} - 2\text{ClO}_4)^{2+}$ 986.27).

X-ray Crystallography. Crystals suitable for X-ray diffraction were obtained by slow diffusion of diethyl ether into CH_2Cl_2 solutions of the Pd complexes. A Bruker Smart 1000 diffractometer equipped with a CCD detector was used for data collection. An empirical absorption correction was applied using the SADABS program. The structure was solved by direct methods and refined by full-matrix least-squares calculations on F^2 using the Shelx1 97 program package.⁸

Crystal data for **4**: $\text{C}_{60}\text{H}_{41}\text{ClN}_4\text{OPd}\cdot\text{CH}_2\text{Cl}_2\cdot\text{H}_2\text{O}$, $M_r = 1078.76$, monoclinic, space group $P2_1/c$ (No. 14), $a = 11.8443(10)$ Å, $b = 18.6502(15)$ Å, $c = 24.072(2)$ Å, $\beta = 103.482(2)^\circ$, $V = 5170.9(7)$ Å³, $Z = 4$, $D_{\text{calcd}} = 1.386$ g/cm³, $\mu(\text{Mo K}\alpha) = 0.562$ mm⁻¹, $T = 293$ K, crystal size $0.3 \times 0.2 \times 0.1$ mm³. A total of 10 269 unique reflections ($2.8 < 2\theta < 54.5^\circ$) were collected, and 648 parameters were refined. All the non-hydrogen atoms

(8) Sheldrick, G. M. SHELX1 5.10 for Windows NT: Structure Determination Software Programs; Bruker Analytical X-ray Systems, Inc., Madison, WI, 1997.

Scheme 1



were refined anisotropically, and the coordinates and U_{ij} values of two water hydrogens were refined. $R1 = 0.0576$, $wR2 = 0.1571$ for 6715 reflections with $I > 2\sigma(I)$; $R1 = 0.0967$, $wR2 = 0.1812$ for all data. GOF on $F^2 = 1.003$.

Crystal data for **5**: $\text{C}_{60}\text{H}_{41}\text{ClN}_4\text{O}_5\text{Pd}\cdot(\text{C}_4\text{H}_{10}\text{O})$, $M_r = 1113.94$, triclinic, space group $P\bar{1}$ (No. 2), $a = 12.1606(13)$ Å, $b = 13.6413(15)$ Å, $c = 16.8606(18)$ Å, $\alpha = 107.800(2)^\circ$, $\beta = 98.264(2)^\circ$, $\gamma = 90.747(2)^\circ$, $V = 2630.6(5)$ Å³, $Z = 2$, $D_{\text{calcd}} = 1.406$ g/cm³, $\mu(\text{Mo K}\alpha) = 0.462$ mm⁻¹, $T = 135$ K, crystal size $0.3 \times 0.1 \times 0.04$ mm³. A total of 10 168 unique reflections ($2.6 < 2\theta < 54.6^\circ$) were collected, and 694 parameters were refined. All the non-hydrogen atoms were refined anisotropically. The refined structure contains a disorder of $\text{Pd}(\text{C}(59\text{A})\text{H}_3)(\text{C}(60\text{A})\text{O}(1\text{A}))$ and $\text{Pd}(\text{C}(59\text{B})\text{H}_3)(\text{C}(60\text{B})\text{O}(1\text{B}))$ moieties with occupancies of 0.587 and 0.413, respectively. In the refinement, C(59) represents both C(59A) and C(60B), whereas C(60) represents both C(59B) and C(60A). $R1 = 0.0616$, $wR2 = 0.1376$ for 6699 reflections with $I > 2\sigma(I)$; $R1 = 0.1018$, $wR2 = 0.1631$ for all data. GOF on $F^2 = 0.942$.

Results and Discussion

Formation and Properties of the (methyl)Pd Complexes of the Bidentate Porphyrin: N^{21},N^{22} -(1,2-Diphenylethene)-*meso*-tetraphenylporphyrin (1**)^{6b}** was quantitatively metalated with $\text{Pd}(\text{Me})(\text{Cl})(\text{cyclo-octadiene})^{2b,7}$ to give $\text{Pd}(\text{Me})(\text{Cl})(\text{por})$ (**2**), where por stands for **1**. The complex **2** was converted into the cationic Pd complex $[\text{Pd}(\text{Me})(\text{por})(\text{MeCN})]\text{ClO}_4$ (**3**) quantitatively by treatment with AgClO_4 in acetonitrile (Scheme 1). The ^1H NMR signals due to the Pd–Me protons of **2** and **3** at -4.13 and -4.35 ppm, respectively, are unambiguously assigned, owing to the porphyrin ring current effect. The singlet at 0.96 ppm due to the coordinated acetonitrile of **3** is also in the lower frequency region in comparison with that of the free acetonitrile at 2.01 ppm in CDCl_3 solution. The complex **2** reacted with CO under atmospheric pressure to give the (acetyl)(chloro)Pd complex $\text{Pd}(\text{C}(\text{O})\text{Me})(\text{Cl})(\text{por})$ (**4**), in 85% isolated yield. The monitoring of this reaction by ^1H NMR indicated that the Pd–Me resonance at -4.13 ppm was replaced by the Pd–C(O)Me resonance at -1.27 ppm without any transient resonances. On the other hand, three new singlets at -4.09 , -1.25 , and -0.45 ppm appeared in the course of the reaction of the cationic complex **3** with CO in CDCl_3 , as shown in Figure 1. The last two signals at around -1 ppm are assigned to the Pd–C(O)Me protons. Since the singlet at -1.25 ppm due to Pd–C(O)Me is accompanied by the singlet at 1.03 ppm due to the coordinated CH_3CN with the same integral, these signals are associated with the cationic (acetyl)Pd complex $[\text{Pd}(\text{C}(\text{O})\text{Me})(\text{por})(\text{MeCN})]$ –

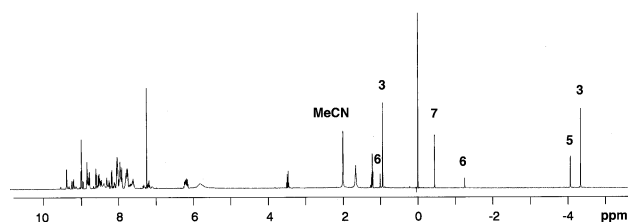
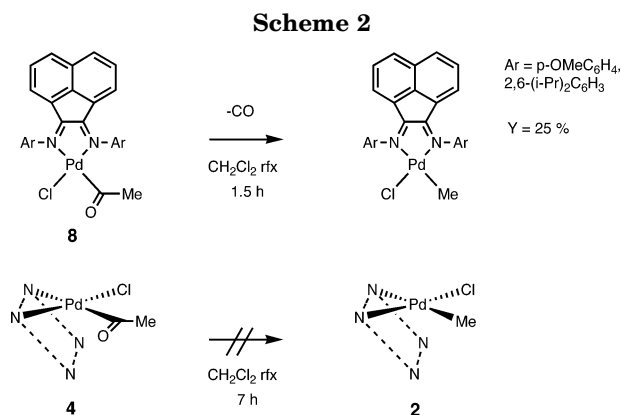


Figure 1. ^1H NMR spectrum of a mixture of $[\text{Pd}(\text{Me})(\text{por})(\text{MeCN})]\text{ClO}_4$ (**3**), $[\text{Pd}(\text{Me})(\text{por})(\text{CO})]\text{ClO}_4$ (**5**), $[\text{Pd}(\text{C}(\text{O})\text{Me})(\text{por})(\text{MeCN})]\text{ClO}_4$ (**6**), and $[\text{Pd}(\text{C}(\text{O})\text{Me})(\text{por})(\text{CO})]\text{ClO}_4$ (**7**).



ClO₄ (**6**). The signals at -4.35 , -4.09 , and -1.25 ppm disappeared by bubbling CO gas to give a single product showing a singlet at -0.45 ppm. This signal is associated with the cationic (acetyl)Pd complex $[\text{Pd}(\text{C}(\text{O})\text{Me})(\text{por})(\text{CO})]\text{ClO}_4$ (**7**). However, the complex **7** readily lost one CO molecule in the course of the workup process to give $[\text{Pd}(\text{Me})(\text{por})(\text{CO})]\text{ClO}_4$ (**5**) in 96% isolated yield. The ^1H NMR signal at -4.09 ppm was associated with the Pd–Me protons of **5**. This reversible insertion and extrusion of CO in the cationic complex is in contrast to the stable (acetyl)(chloro)Pd complex **4**, that did not change at all under reflux in CH_2Cl_2 for 7 h. A cationic intermediate complex, $[\text{Pd}(\text{Me})(\text{por})(\text{CO})]\text{Cl}$, structurally similar to **5** may be involved in the CO insertion reaction of **2** to **4**. Since the Cl^- ion is poorly solvated in CH_2Cl_2 , it would occupy the coordination site of Pd(II) to give the stable complex **4**. This explanation is consistent with the fact that the CO ligand of **5** was not simply replaced by MeCN but rendered to insert into the Pd–Me bond, leading to **6**, when excess MeCN was added to a CDCl_3 solution of **5** in the absence of CO.

These reaction behaviors of the Pd complexes of the bidentate porphyrin are in remarkable contrast to the CO insertion reaction of the (methyl)Pd complexes with bidentate nitrogen donor ligands such as bis(arylimino)acenaphthene (Ar-BIAN) and phenanthroline (phen).^{9–12}

(9) van Asselt, R.; Gielens, E. E. C. G.; Rulke, R. E.; Vrieze, K.; Elsevier, C. J. *J. Am. Chem. Soc.* **1994**, *116*, 977.

(10) Bastero, A.; Ruiz, A.; Claver, C.; Milani, B.; Zangrando, E. *Organometallics* **2002**, *21*, 5820.

(11) (a) Rix, F. C.; Brookhart, M. *J. Am. Chem. Soc.* **1995**, *117*, 1137. (b) Rix, F. C.; Brookhart, M.; White, P. S. *J. Am. Chem. Soc.* **1996**, *118*, 4746. (c) Ledford, J.; Shultz, C. S.; Gates, D. P.; White, P. S.; DeSimone, J. M.; Brookhart, M. *Organometallics* **2001**, *20*, 5266. (d) Shen, H.; Jordan, R. F. *Organometallics* **2003**, *22*, 1878.

(12) (a) Rülke, R. E.; Delis, J. G. P.; Groot, A. M.; Elsevier, C. J.; van Leeuwen, P. W. N. M.; Vrieze, K.; Goubitz, K.; Schenk, H. *J. Organomet. Chem.* **1996**, *508*, 109. (b) Delis, J. G. P.; Aubel, P. G.; Vrieze, K.; van Leeuwen, P. W. N. M.; Veldman, N.; Spek, A. L.; van Neer, F. J. R. *Organometallics* **1997**, *16*, 2948. (c) van Asselt, R.; Vrieze, K.; Elsevier, C. J. *J. Organomet. Chem.* **1994**, *480*, 27.

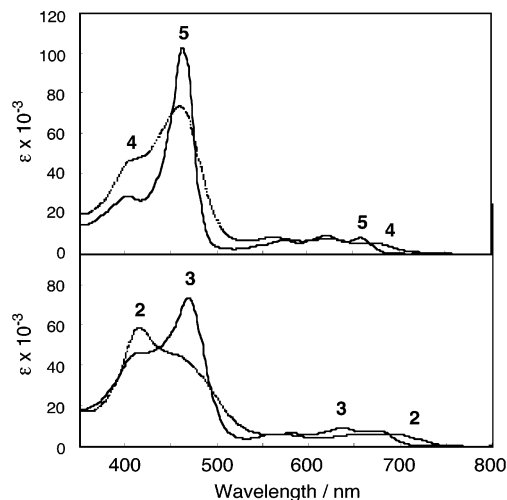


Figure 2. UV–vis spectra of $\text{Pd}(\text{CH}_3)(\text{Cl})(\text{por})$ (**2**), $[\text{Pd}(\text{CH}_3)(\text{por})(\text{CH}_3\text{CN})]\text{ClO}_4$ (**3**), $\text{Pd}(\text{C}(\text{O})\text{CH}_3)(\text{Cl})(\text{por})$ (**4**), and $[\text{Pd}(\text{CH}_3)(\text{por})(\text{CO})]\text{ClO}_4$ (**5**) in CH_2Cl_2 .

It was reported that $\text{Pd}(\text{C}(\text{O})\text{Me})(\text{Cl})(\text{Ar-BIAN})$ (**8**) was decarbonylated to give the $\text{Pd}(\text{Me})(\text{Cl})$ complex in 25% yield after reflux in CH_2Cl_2 for 1.5 h (Scheme 2).⁹ Furthermore, the $[\text{Pd}(\text{C}(\text{O})\text{Me})(\text{CO})]^+$ and $[\text{Pd}(\text{C}(\text{O})\text{Me})(\text{MeCN})]^+$ complexes were obtained through bubbling CO gas into a solution of the cationic complex $[\text{Pd}(\text{Me})(\text{Ar-BIAN})(\text{MeCN})]\text{CF}_3\text{SO}_3$ at 20 °C, followed by evaporation of the solvent.⁹ A detailed NMR study on the CO insertion process in the cationic $[\text{Pd}(\text{Me})(\text{MeCN})]^+$ complexes of the bidentate pyridine–imidazoline ligands has shown a reaction sequence similar to the CO insertion of **3**.¹⁰ However, the $[\text{Pd}(\text{C}(\text{O})\text{Me})(\text{CO})]^+$ complexes are always stable and do not go back to the $[\text{Pd}(\text{Me})(\text{CO})]^+$ complexes by releasing CO. Therefore, the latter complexes were able to be prepared from the $[\text{Pd}(\text{Me})(\text{L})]^+$ complexes only by reacting a limited amount of CO at temperatures below -78 °C, thereby suppressing formation of the $[\text{Pd}(\text{C}(\text{O})\text{Me})(\text{CO})]^+$ complexes.¹¹ In comparison with these previous reports on the formation of the (carbonyl)(methyl)Pd complexes, the easy preparation and good stability of the $[\text{Pd}(\text{Me})(\text{por})(\text{CO})]^+$ complex **5** at room temperature is noteworthy. The CO stretching band at 2099 cm^{-1} in the IR spectrum of **5** is at a significantly lower frequency than the $\nu(\text{CO})$ values in the range of 2120 – 2140 cm^{-1} reported for the cationic (carbonyl)(methyl)Pd and (acetyl)(carbonyl)Pd complexes.¹¹ Therefore, π -back-donation from Pd to the CO ligand seems very important in stabilizing the complex **5**. It means that the π -accepting ability of the bidentate porphyrin ligand is weaker than that of the diphosphine and phenanthroline ligands. This may be explained in terms of the distorted coordination structure that the Pd–N_{pyrrole} bonds of **5** are bent by ca. 20° from the corresponding mean pyrrole planes (vide infra). It is also considered that the electron-donating effect from the N-substituted pyrrole nitrogens by way of the π -conjugation system can strengthen the σ -donating ability of the imine-type pyrrole nitrogens to Pd.

The UV–visible spectra of **2**–**5** show two absorption bands at around 410 and 465 nm in the Soret region, as shown in Figure 2. The cationic Pd complexes **3** and **5** show a stronger band in the 465 nm region than the corresponding neutral complexes **2** and **4**, respectively. There are considerable differences among these four

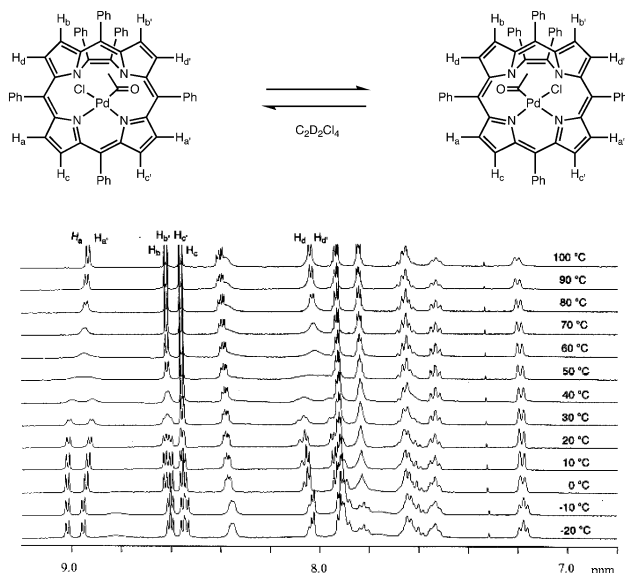
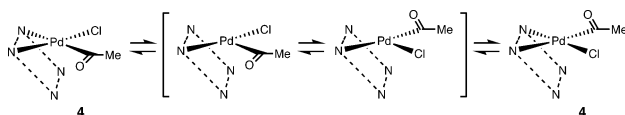


Figure 3. Variable-temperature ^1H NMR spectra of $\text{Pd}(\text{C}(\text{O})\text{CH}_3)(\text{Cl})(\text{por})$ (**4**) in $\text{C}_2\text{D}_2\text{Cl}_4$.

Scheme 3



complexes in the spectral patterns of the visible region as well as of the Soret region. It is remarkable that the UV–visible bands of the bidentate porphyrin ligand are sensitive to the nature of the rest of the two ligands on Pd. The ^1H NMR signals due to the β -pyrrole protons of **4** show temperature-dependent broadening, while a very sharp singlet due to the Pd–acetyl protons is unchanged. The variable-temperature NMR measurement of **4** in $\text{C}_2\text{D}_2\text{Cl}_4$ (Figure 3) indicates that the eight different signals of the β -pyrrole protons coalesce at 50 $^\circ\text{C}$ into the four signals at 8.01, 8.54, 8.60, and 8.88 ppm at higher temperatures. This spectral change is explained in terms of the site exchange between the acetyl ligand and the Cl ligand. The estimated ΔG^\ddagger_{323} value (68 kJ mol^{-1}) on the basis of the coalescence temperature of the β -pyrrole proton signals at 9.2 and 8.8 ppm at 30 $^\circ\text{C}$ is smaller than the value ($\Delta G^\ddagger_{323} = \sim 75$ kJ mol^{-1}) reported for a similar site exchange process of the bipyridine (bpy) complexes $\text{Pd}(\text{C}(=\text{N}-t\text{-Bu})\text{Me})(\text{Cl})(\text{bpy})$ and $\text{Pd}(\text{C}(\text{O})\text{Me})(\text{Cl})(\text{bpy})$ (**9**).¹² In fact, these data were determined by the spin saturation transfer method because the exchange rate is slower than the present case.¹³

This acetyl-chloro site exchange has generally been explained in terms of the dissociation of one Pd–N bond, the ligand rotation around the remaining Pd–N bond, and the recombination of a Pd–N bond (see Scheme 3).^{12a} We have shown that the apparent π -allyl ligand rotation of $[\text{Pd}(\pi\text{-allyl})(\text{por})]\text{ClO}_4$ takes place through a Pd–N bond dissociation mechanism, where the ΔG^\ddagger_{298} value (91.2 kJ mol^{-1}) is more than 20 kJ mol^{-1} greater than those of the (π -allyl)Pd complexes of the bidentate

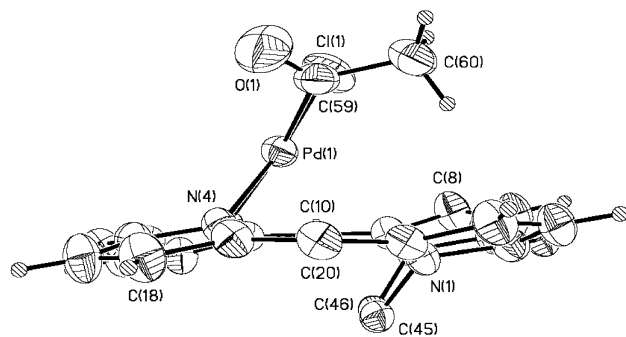
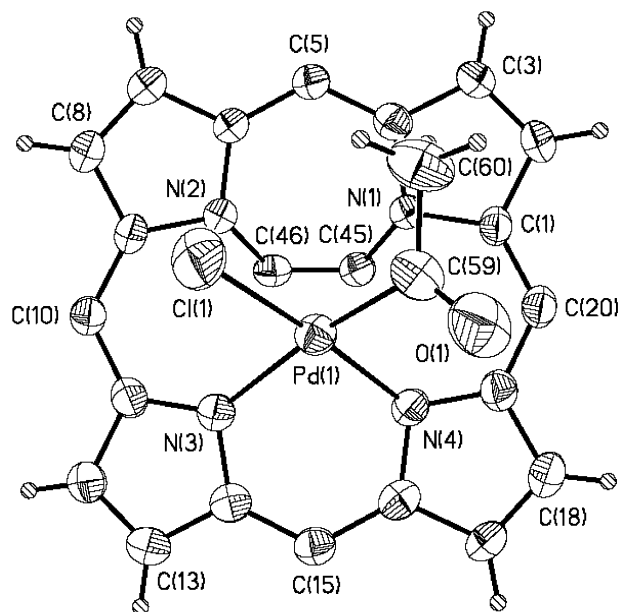
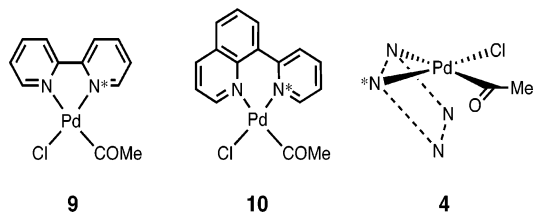


Figure 4. The X-ray structure (top and side views) of $\text{Pd}(\text{C}(\text{O})\text{Me})(\text{Cl})(\text{por})$ (**4**) with the atom-numbering scheme. Six phenyl groups at C5, C10, C15, C20, C45, and C46 were omitted for clarity.

nitrogen ligands such as bipyridine.^{6d} The smaller ΔG^\ddagger value for the acetyl–chloro site exchange of **4** as compared to that of **9** is in contrast to the greater ΔG^\ddagger value for the apparent π -allyl ligand rotation of the Pd(por) complex as compared to that of the Pd(bpy) complex. It seems that the steric constraint between the acetyl ligand and the bidentate porphyrin ligand lowers the ΔG^\ddagger value in the acetyl–chloro site exchange of **4**, as discussed later.

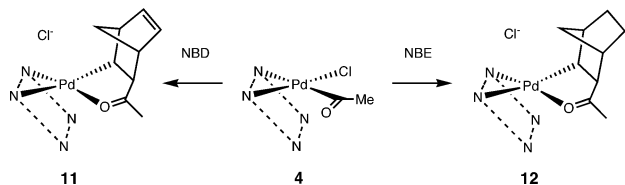
In the X-ray structure of **4** shown in Figure 4, the N(3)N(4)Pd plane is canted by 55.2 $^\circ$ from the mean porphyrin plane that is defined by the four meso carbons, C(5), C(10), C(15), and C(20). Four pyrrole planes are tilted from the mean porphyrin plane by 12–19 $^\circ$. Two pyrroles coordinating to Pd are tilted in the opposite direction to the two pyrroles having the diphenylethene bridge. These structural features are very similar to those of the $[\text{Pd}(\pi\text{-allyl})(\text{por})]\text{ClO}_4$ complex.^{6c} The carbonyl oxygen of the acetyl ligand of **4** is at an anti position relative to the chloro ligand, and thus the methyl group is sitting at the region where a strong ring current effect of the bidentate porphyrin would be induced. This structure can be directly compared with that of the analogous Pd complexes **9** and **10** with the bipyridine ligand and the pyridylquinoline ligand, respectively, in Table 1.^{12a,14a} It is reasonable both for **4** and **10** that the Pd–N* bond trans to the Pd–Cl bond

(13) (a) Crabtree, R. H. *The Organometallic Chemistry of the Transition Metals*; Wiley: New York, 1988. (b) Kaplan, J. I.; Fraenkel, G. *NMR of Chemically Exchanging Systems*; Academic Press: New York, 1980.

Table 1. Bond Lengths (Å), Bond Angles (deg) and Torsion Angles (deg) of Pd(C(O)Me)(Cl)(N \wedge N) Complexes^a


	9	10	4
Pd–C	1.948	1.953	1.948(5)
Pd–Cl	2.320	2.327	2.322(1)
C=O	1.196	1.225	1.205(6)
Pd–N	2.162	2.187	2.213(4)
Pd–N*	2.067	2.060	2.084(4)
N–Pd–N*	77.73	86.58	83.35(14)
C–Pd–Cl	88.47	86.50	88.00(17)
N–Pd–Cl	97.25	91.61	95.47(11)
N*–Pd–C	96.53	95.33	92.7(2)
N*–Pd–C=O	–66.16	–74.64	–54.04

^a Taken from ref 12a for **9** and ref 14a for **10**.

Scheme 4

is shorter than the Pd–N bond trans to the acetyl ligand. The longer Pd–N bond is bent by 30.9° from the coordinating quinoline plane (defined by three atoms, C_α–N–C_{α'}), whereas the shorter Pd–N* bond is bent only by 4.8° from the coordinating pyridine plane (defined by three atoms, C_α–N–C_{α'}) in the case of **10**. In contrast, the shorter Pd–N(4) bond of **4** is bent by a greater degree (27.6°) than the longer Pd–N(3) bonds of **4** (20.7°) with respect to the corresponding mean pyrrole planes. Furthermore, the torsion angle N(4)–Pd–C(59)=O(1) of **4** (–54.04°) is smaller than the corresponding torsion angles of **9** (–66.16°) and **10** (–74.64°). These structural features are indicative of the steric constraint between the acetyl ligand and the bidentate porphyrin ligand, which may be responsible for the remarkable thermodynamic stability of the (carbonyl)(methyl)Pd complex **5** over the (acetyl)Pd complexes **6** and **7**. Only a few X-ray crystal structures have so far been reported for the mononuclear Pd complexes coordinated both by the carboanionic ligand and carbon monoxide such as the ionic complexes [Pd(3-nitro-2-tolyl)(Cl)₂(CO)][–] and [Pd(C(O)Me)(phen)(CO)]⁺.^{11b,15} Complex **5** is the first example of a Pd(Me)–

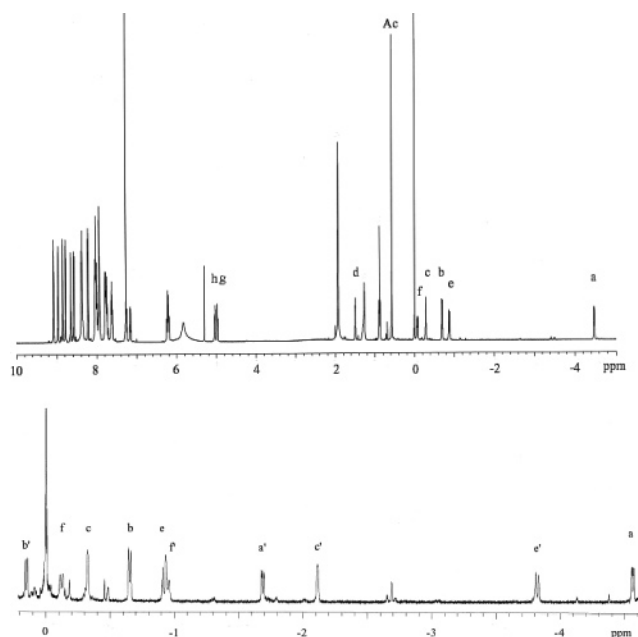


Figure 5. ¹H NMR spectra of Pd(C₇H₈C(O)Me)(Cl)(por) (**11**) (top) and a mixture of the corresponding perchlorates **13a** and **13b** at 0 °C (bottom). See Table 2 for the signal assignments. Signals designated as a', b', c', e', and f' are associated with **13b**.

(CO) complex characterized by X-ray crystallography, although there was a positional disorder between the CO ligand and the Me ligand (see the Supporting Information). The X-ray structure of the cationic (ethylene)(methyl)Pd complex that is also a preinsertion model complex has recently been reported.¹⁶

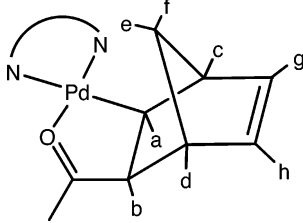
Reactions of the (methyl)Pd Complexes with Norbornadiene. While the (methyl)Pd complex **2** did not react at all with norbornadiene (NBD) (10 equiv) at room temperature for several days, the (acetyl)Pd complex **4** gradually reacted with NBD and norbornene (NBE) at room temperature in 1 or 2 days to give the insertion products **11** and **12** in 96% and 81% yields, respectively (Scheme 4). The ¹H NMR spectrum of the NBD insertion complex **11** shows signals due to the Pd-bound organic group at frequency regions significantly influenced by the porphyrin ring current effect (see Figure 5, top). Two singlets at –0.29 and 1.49 ppm are associated with the bridgehead methine protons (H_c and H_d) of the norbornene moiety. A pair of doublets at –0.88 and –0.07 ppm with a geminal coupling constant of 8.4 Hz are assigned to the CH₂ bridge protons (H_e and H_f), and a pair of doublets at –4.48 and –0.69 ppm with a vicinal coupling constant of 6.4 Hz are assigned to the two-carbon bridge protons (H_a and H_b) of the norbornene framework, as summarized in Table 2. Since the vicinal coupling constant (*J*_{ab} = 6.4 Hz) for the Pd–CH_a–CH_b–C(O)Me moiety is a typical value between the endo protons of the norbornene framework,¹⁷ it is deduced that the addition of Pd and the acetyl group occurred on the exo side of NBD. This stereochemistry is further supported by the smallest ring current effect on the –CH=CH– bridge protons (H_g and H_h) at 4.97

(14) (a) Delis, J. G. P.; Rep, M.; Rulke, R. E.; van Leeuwen, P. W. N. M.; Vrieze, K.; Fraanje, J.; Goubitz, K. *Inorg. Chim. Acta* **1996**, *250*, 87. Related X-ray structures of Pd(C(O)Me)(Cl)(N \wedge N) complexes: (b) Elguero, J.; Guerrero, A.; de la Torre, F. G.; de la Hoz, A.; Jalon, F. A.; Manzano, B. R.; Rodriguez, A. *New J. Chem.* **2001**, *25*, 1050. (c) Pelagatti, P.; Carcelli, M.; Franchi, F.; Pelizzi, C.; Bacchi, A.; Fochi, A.; Fruhauf, H.-W.; Goubitz, K.; Vrieze, K. *Eur. J. Inorg. Chem.* **2000**, 463. (d) Groen, J. H.; Vlaar, M. J. M.; van Leeuwen, P. W. N. M.; Vrieze, K.; Kooijman, H.; Spek, A. L. *J. Organomet. Chem.* **1998**, *551*, 67.

(15) (a) Vicente, J.; Arcas, A.; Borrachero, M. V.; Tiripicchio, A.; Camellini, M. *Organometallics* **1991**, *10*, 3873. (b) Ara, I.; Fornies, J.; Navarro, R.; Sicilia, V.; Urriolaibeitia, E. P. *Polyhedron* **1997**, *16*, 1963.

(16) Malinoski, J. M.; White, P. S.; Brookhart, M. *Organometallics* **2003**, *22*, 621.

(17) Brumbaugh, J. S.; Whittle, R. R.; Parvez, M.; Sen, A. *Organometallics* **1990**, *9*, 1735.

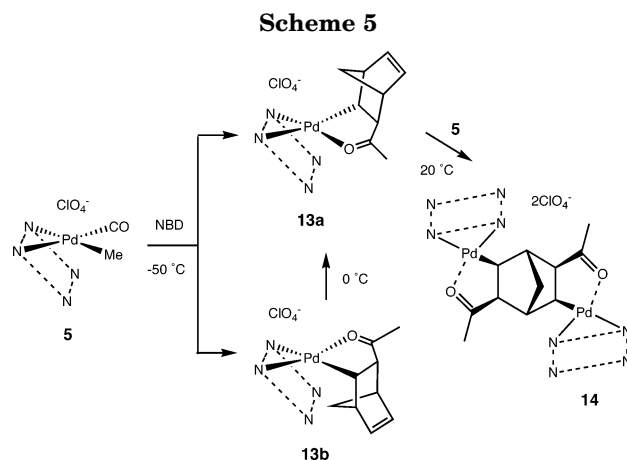
Table 2. ^1H NMR Chemical Shifts (δ , in CDCl_3) of the Pd–Alkyl Group of the Insertion Products 11–14


	11	12	13a	13b ^a	14
a	-4.48	-4.05	-4.51	-1.69	-4.59
b	-0.69	-0.51	-0.61	0.15	-1.70
c	-0.29	-1.07	-0.31	-2.11	-1.81
d	1.49	0.84	1.48	1.42	
e	-0.88	-0.69	-0.91	-3.82	-2.65
f	-0.07	-0.19	-0.11	-0.95	
g	4.97	-0.35, 0.42 ^b	4.95	4.77	
h	5.04	0.02, 0.60 ^b	5.06	5.04	
Ac	0.58	0.58	0.58	0.82	0.21

^a Measured at 0 °C. ^b Methylene protons.

and 5.04 ppm. The considerably low frequency of the acetyl protons at 0.58 ppm despite the δ -carbon position with respect to Pd is indicative of the coordination of the acetyl oxygen to Pd. This acetyl coordination is further supported by the CO stretching frequencies at 1624 and 1598 cm^{-1} in the IR spectrum of **11**, which are in good agreement with that (1603 cm^{-1}) reported for an analogous NBD insertion complex of Pd(bpy).^{18a} A 1710 cm^{-1} band also observed in the IR spectrum of **11** is indicative of the acetyl coordination equilibrium. A spectral feature very similar to that of **11** was observed for the NBE insertion complex **12**, except that the bridgehead methine protons (H_c and H_d) are shifted to 0.78 and 0.65 ppm lower frequency and the vinyl proton signals of **11** at ca. 5 ppm were replaced by methylene proton signals appearing between 0.60 and -0.35 ppm, as summarized in Table 2.

The (carbonyl)(methyl)Pd complex **5** reacted rapidly with NBD to give the insertion complex **13a** in 91% yield (Scheme 5). The ^1H NMR spectra of **11** and **13a** are substantially the same, with the chemical shift differences being less than 0.08 ppm (see Table 2). When the reaction of **5** and NBD (5 equiv) in CDCl_3 was monitored by ^1H NMR, the formation of a 1:1 mixture of **13a** and its isomer **13b** was complete within 5 min at -50 °C. While the coupling patterns of the signals due to the Pd-bound organic groups of **13a** and **13b** are almost identical, their chemical shifts are quite different (see Figure 5, bottom). The bridge CH_2 signals (H_e and H_f) shifted from -0.91 and -0.11 ppm for **13a** to -3.82 and -0.95 ppm for **13b**, in contrast to the high-frequency shifts of the proton signals due to the Pd- CH_a - CH_b -C(O)Me moiety from -4.51 and -0.61 ppm for **13a** to -1.69 and 0.15 ppm for **13b**. These NMR features are consistent with the structures depicted in Scheme 5, where the porphyrin plane is close to the bridge CH_2 in



the case of **13b** and close to the endo protons of the Pd- CH_a - CH_b -C(O)Me moiety in the case of **13a**. The complex **13b** began to be converted into **13a** at temperatures higher than 0 °C. The dissociation of the carbonyl oxygen allows rotation of the norbornenyl moiety around the Pd-C bond in the three-coordinate intermediate. Alternatively, the above isomerization can be explained in terms of the rotation of the bidentate porphyrin ligand around the Pd-N bond following the dissociation of one Pd-N bond. The reaction of NBD with 2-fold molar amounts of **5** afforded the dipalladium complex **14** in 92% yield. The double cis-exo addition to NBD was confirmed by the coupling constant (6.0 Hz) of the Pd- CH_a - CH_b -C(O)Me moiety, the chelate structure of which is indicated by a strong CO stretching band at 1612 cm^{-1} .¹⁸ The C_2 -symmetric structure of **14** was evidenced by the appearance of a single absorption due to the bridgehead methine protons (H_c and H_d) at -1.81 ppm.

Conclusion

We have shown in this paper the chemistry of the (methyl)Pd complexes of the bidentate porphyrin ligand with unique electronic and stereochemical features. The ^1H NMR spectroscopic investigation is very useful, owing to the bidentate porphyrin ligand in analyzing structures and reactions of the Pd complexes. Since the cationic (carbonyl)(methyl)Pd complex is stabilized by this bidentate porphyrin ligand, it was able to be prepared quantitatively after bubbling a large excess of CO gas at room temperature. This is remarkable in view of the fact that rigorous control of the amount of CO and temperature below -78 °C was needed in the case of the previously reported (carbonyl)(methyl)Pd complexes. The steric constraint between the acetyl ligand and the bidentate porphyrin ligand was seen in the X-ray structure of the (acetyl)Pd complex, and it seems to provide great influence on the CO insertion reaction of the cationic (methyl)Pd complex and on the acetyl-chloro site exchange in the (chloro)(acetyl)Pd complex. The cationic (carbonyl)(methyl)Pd complex underwent rapid insertion of norbornadiene, and the rotation of the resulting (organo)Pd moiety was observed at temperatures higher than 0 °C.

(18) (a) Markies, B. A.; Kruis, D.; Rietveld, M. H. P.; Verkerk, K. A. N.; Boersma, J.; Kooijman, H.; Lakin, M. T.; Spek, A. L.; van Koten, G. *J. Am. Chem. Soc.* **1995**, *117*, 5263. (b) Spek, A. L.; Markies, B. A.; Kruis, D.; Boersma, J.; van Koten, G. *Acta Crystallogr., Sect. C* **1995**, *51*, 1535. (c) Markies, B. A.; Rietveld, M. H. P.; Boersma, J.; Spek, A. L.; van Koten, G. *J. Organomet. Chem.* **1992**, *424*, C12.

Acknowledgment. This work was supported by a grant-in-aid for scientific research (No. 12440186) from the Ministry of Education, Science, Sports, and Culture of Japan. We thank Ms. M. Nishinaka (Kobe University) for analytical work.

Supporting Information Available: Crystallographic data for **4** and **5** with their Ortep drawings. This material is available free of charge via the Internet at <http://pubs.acs.org>.

OM049783D